NEW EVIDENCE FOR SURFACE WATER ICE IN SMALL-SCALE COLD TRAPS AND IN THREE LARGE CRATERS AT THE NORTH POLAR REGION OF MERCURY FROM THE MERCURY LASER ALTIMETER. Ariel N. Deutsch[1], Gregory A. Neumann[2], and James W. Head[1], [1]Department of Earth, Environmental and Planetary Sciences, Brown University, Providence, RI 02912 (ariel_deutsch@brown.edu), [2]NASA Goddard Space Flight Center, Greenbelt, MD 20771, USA.

Introduction: Earth-based radar images of Mercury first revealed highly reflective materials that are consistent with water ice [e.g., 1–2]. These "radar-bright" materials collocate with permanently shadowed regions (PSRs) [e.g., 3–4], which are stable environments for near-surface and sometimes surface water ice on geologic timescales [5]. Enhanced concentrations of hydrogen have been detected in the north polar region on Mercury, consistent with a water ice composition [6].

The Mercury Laser Altimeter (MLA) instrument onboard the MErcury Surface, Space ENvironment, GEochemistry, and Ranging (MESSENGER) spacecraft measured the surface reflectance at 1064 nm at zero phase angle across the northern hemisphere of Mercury. The surface reflectance within PSRs is anomalously lower or higher than the average reflectance of Mercury [7]. Reflectance anomalies correlate with areas that thermal models predict are environments capable of hosting stable water ice [5]. Typically, water ice on Mercury is insulated by a layer of low-reflectance materials, which is estimated to be 10–30 cm thick on the basis of comparative variation of the flux of epithermal and fast neutrons with latitude [6].

In contrast to low-reflectance deposits, which are suggestive of subsurface ice, high-reflectance deposits are indicative of surface water ice [7]. MLA reflectance [7] and MDIS-scattered-light imaging [8] observations revealed one such high-reflectance surface on the floor of Prokofiev crater (85.8°N, 62.9°E). The anomalously high-reflectance deposit collocates with radar-bright material [2]. Thermal models [5] indicate that the floors of some higher-latitude craters, including Prokofiev, can support water ice exposed at the surface for billions of years without the need for an insulating layer. Here we have investigated these craters using newly calibrated MLA reflectance data [9].

Given that surface reflectance increases northward of ~85°N [9] and that micro-cold traps may be ubiquitous at latitudes northward of ~75°N [10–11], we are interested in the detection of exposures of water-ice deposits present at the surface of Mercury at small spatial scales. Following the Earth-based identification of high radar-backscatter deposits in polar craters, the only detections of exposed water ice have been in large, permanently shadowed craters: Prokofiev crater [7–8], as well as limited off-nadir MLA measurements of A, C, D2, Kandinsky, i5, and Y craters [7] (**Fig. 1**) (For craters that do not have formal IAU names, we adopt informal nomenclature from published maps). Here we investigate the presence of specific small-scale cold traps by searching for clustered MLA-measured surface reflectance, r_s, enhancements at 1064-nm wavelength that can be observed at the resolution of MLA footprints, and discuss the implications of small-cold traps on Mercury's total ice budget.

We also map r_s and the density of energy returns in Chesterton, Tolkien, and Tryggvadóttir craters. Like Prokofiev, these three permanently shadowed craters host extensive radar-bright deposits indicative of water ice [2]. However, MESSENGER only acquired limited off-nadir observations of these craters due to their proximity to the pole. The nominally calibrated r_s measurements of these craters did not show distinctive regions of $r_s > 0.3$ in contrast to those in Prokofiev acquired at a more favorable geometry. The greater density of returns observed within the PSRs prompted a reexamination of the calibration to account for a downward bias due to highly oblique geometry [9]. Utilizing the complete orbital dataset and empirically re-calibrated data, we calculate the mean r_s within the craters and outside the craters, and discuss the implications for surface water-ice deposits hosted by permanently shadowed craters on Mercury.

Methods: *Small-scale cold traps.* Using publicly available data covering Mission Years 1–4, we produced a map of surface reflectance at a wavelength of 1064 nm of the north polar region from 82.5°N to 90°N at zero phase angle, producing a photometrically uniform data set (Fig. 1) [9]. All data analyzed in this paper are available on the NASA Planetary Geodynamics Data Archive (pgda.gsfc.nasa.gov). With the empirically recalibrated map of r_s values, we searched for clusters of pulses that show reflectance enhancements, where $r_s > 0.3$, suggestive of exposed water ice. We then compared any areas that show r_s enhancements to areas with radar-bright material [2], permanent shadow [4], and where $T_{max} < 100$ K [5], indicating the presence of exposed water ice.

Large craters. We mapped measurements of surface reflectance, r_s, at 1064-nm in Chesterton, Tolkien, and Tryggvadóttir. We calculated the mean r_s

values inside and outside each crater for a range of 2R, where R is the radius of the crater. For each crater, we determined if there was a substantial deviation in reflectance between the crater floor and the surrounding terrain.

Exposures of surface water ice: *Small-scale cold traps.* We identified four clusters of MLA pulses that have values of $r_s > 0.3$. These four clusters are located in small-scale cold traps, in small yet resolvable areas that are between 2 and 5 km in diameter, in craters n5, o7, l7, and to the north of e5 (Fig. 1). These small-scale cold traps align with regions that thermal stability models predict are capable of sustaining surface ice [5]. Surface reflectance measurements show distinct enhancements in comparison to the surrounding terrains. The high r_s values coincide with PSRs [4] and radar-bright material [2] using a threshold of four standard deviations of the noise.

Large craters. We calculate the mean r_s value inside each crater, while avoiding crater slopes, and the mean r_s value for the area outside each crater, for areas 2-radii from the crater rim. For each of the large craters, the mean r_s inside the crater exceeded 0.3 and is significantly enhanced relative to the exterior mean r_s values. By including only 75% of the crater interior, we avoid crater slopes in our calculations, thus eliminating the likelihood that these reflectance enhancements could be caused by mass wasting.

Micro-cold traps on Mercury: There are likely to be substantially more micro-cold traps that exist below the spatial resolution of MLA. The surface reflectance from ~85°N to 90°N [9] is likely to be enhanced by the presence of micro-cold traps that host spatially small water-ice deposits (< a few km in diameter). This interpretation is consistent with the most recent thermal modeling, which suggests that a large fraction of the ice on Mercury resides inside micro-cold traps distributed along the inter-crater terrain, on the scales of 10–100 m rough patches [10].

In our analysis of the large craters Chesterton, Tolkien, and Tryggvadóttir, the mean surface reflectances outside of these craters were between 0.2776 ± 0.0067 and 0.2836 ± 0.0077, which are values that are enhanced relative to the reflectance of typical mercurian regolith. These regions are not likely to host extensive water-ice deposits due to the low fractional area covered by PSRs and thus the thermal instability of this terrain, but it is possible that such rough terrain close to the pole contains spatially small patches of exposed water ice. These mean values between ~0.25 and ~0.3 suggest that there is a mixture of exposed ice (in micro-cold traps) and regolith present (predominantly outside of the cold traps).

Implications for the ice inventory of Mercury: Thermal models [11] have been used to estimate the total surface area of micro-cold traps in the north polar region of Mercury that is occupied by near-surface water-ice insulated by low-reflectance deposits. However, updated thermal modeling is required for numerical calculations on the percentage of micro-cold traps occupied by exposed water ice. It is reasonable to assume that the fractional area of exposed water ice will increase substantially as well. Thus, current estimates of Mercury's water ice inventories are underestimated without accounting for ice within micro-cold traps. For example, conservative modeling suggests that accounting for micro-cold traps on the Moon doubles the cold-trapping area [12].

References: [1] Slade M. A. et al. (1992) *Science, 258,* 635–640. [2] Harmon J. K. et al. (2011) *Icarus, 211,* 37–50. [3] Chabot N. L. et al. (2012) *GRL, 39,* L09204. [4] Deutsch A. N. et al. (2016) *Icarus, 280,* 158–171. [5] Paige D. A. et al. (2013) *Science, 339,* 300–303. [6] Lawrence D. J. et al. (2013) *Science, 339,* 292–296. [7] Neumann G. A. et al. (2013) *Science, 339,* 296–300. [8] Chabot N. L. et al. (2014) *Geology, 42,* 1051–1054. [9] Neumann G. A. et al. (2017) *LPS XLVIII,* Abstract #2660. [10] Rubanenko L. et al. (2017) *LPS XLVIII,* Abstract #1461. [11] Paige D. A. et al. (2014) *LPS XLV,* Abstract #2501. [12] Hayne P. O. (2015) *NASA ESF,* Abstract #47.

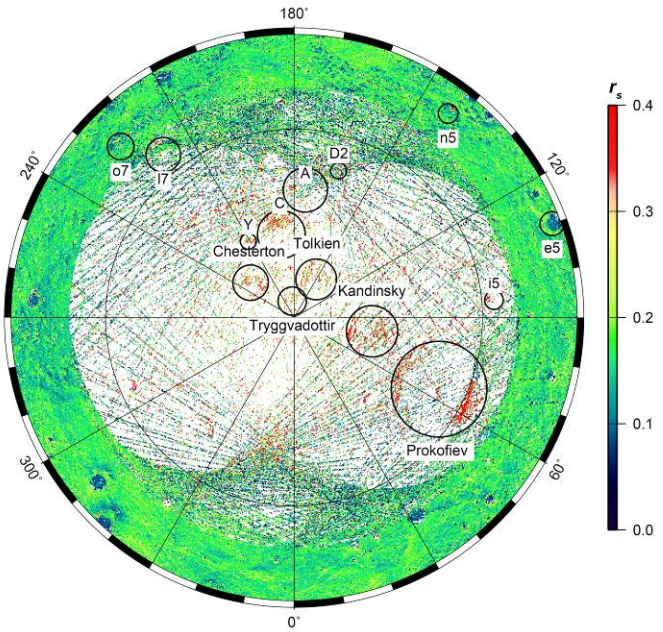

Fig. 1. MLA-derived surface reflectance, r_s, at 1064 nm from 82.5ºN to 90°N, modified from [9]. Large craters (Prokofiev, Chesterton, Tolkien, Tryggvadóttir, Kandinsky, C, Y, and i5) that are identified as hosting exposed water ice are labeled. Small-scale cold traps (n5, o7, e5, and l7) that are identified as hosting exposed water ice are labeled. Polar stereographic projection.